Influence of multi-exciton correlations on nonlinear polariton dynamics in semiconductor microcavities

2013 New J. Phys. 15 025005

(http://iopscience.iop.org/1367-2630/15/2/025005)

New Journal of Physics
The open access journal for physics

Influence of multi-exciton correlations on nonlinear polariton dynamics in semiconductor microcavities

P Wen[1], G Christmann[2], J J Baumberg[2] and Keith A Nelson[1,3]

[1] Department of Chemistry, Massachusetts Institute of Technology, Cambridge, MA 02139, USA

[2] Cavendish Laboratory, University of Cambridge, Cambridge CB3 0HE, UK

E-mail: kanelson@mit.edu

New Journal of Physics **15** (2013) 025005 (14pp)
Received 20 August 2012
Published 5 February 2013
Online at http://www.njp.org/
doi:10.1088/1367-2630/15/2/025005

Abstract. Using two-dimensional spectroscopy, we resolve multi-polariton coherences in quantum wells embedded inside a semiconductor microcavity and elucidate how multi-exciton correlations mediate polariton nonlinear dynamics. We find that polariton correlation strengths depend on spectral overlap with the biexciton resonance and that up to at least four polaritons can be correlated, a higher-order correlation than observed to date among excitons in bare quantum wells. The high-order correlations can be attributed to coupling through the cavity mode, although the role of high-order Coulomb correlations cannot be excluded.

Contents

[3] Author to whom any correspondence should be addressed.

1. Introduction

The correlated dynamics of excitons that are strongly coupled to light, forming exciton–polaritons, is the basis for many intriguing physical phenomena including parametric amplification [1], Bose–Einstein condensation [2] and superfluid behaviour [3]. Correlated Coulomb interactions between pairs of excitations contribute significantly to polariton nonlinear responses [4, 5], but the experimental signatures of Coulomb correlations are usually convolved with those of other nonlinear interactions [6], impeding isolation and understanding of the distinct effects.

Polariton states can be formed by embedding quantum wells (QWs) inside a semiconductor microcavity (SCMC), strongly coupling the QW exciton state and microcavity light mode [7], as shown in figure 1(a). The strong coupling produces upper polariton (UP) and lower polariton (LP) modes. As a consequence of the mixed exciton–photon character, polaritons have extremely low effective mass, giving steeply sloped UP and LP dispersion curves (figures 1(b) and (c)), but they are still influenced by exciton nonlinearities such as Coulomb correlations that arise from interactions between electron and hole constituents of nearby excitons [8, 9]. Besides mean-field repulsive interactions, Coulomb forces can correlate two or more excitons for a finite period of time, resulting in multi-exciton properties and dynamics distinct from those of isolated excitons [10, 11]. In the case of two spin-paired excitons, for example, Coulomb correlations result in a weakly bound biexciton state. Regardless of the spin configuration, two-exciton correlations have been shown to significantly modify polariton nonlinear signal strengths; calculations of polariton scattering magnitudes are incorrect, by orders of magnitude, without including two-exciton correlations [4, 5]. Strong coupling to light modifies two-exciton correlations by altering the resonance frequencies from those of the constituent excitons. Although they play key roles, coherent exciton–polariton pairs or higher-order correlations have never been observed directly.

Recently, there has been substantial progress detailing multi-exciton correlations in QWs using two-dimensional Fourier transform optical spectroscopy (2D FT OPT) [12–16]. 2D FT OPT is an extension of 1D forms of nonlinear spectroscopy, such as time-resolved and time-integrated four-wave mixing (FWM), that have been applied to study many-body physics in semiconductors for over 20 years. As reviewed by Chemla and Shah [6], experiments using 1D nonlinear spectroscopy clearly demonstrated the importance of multi-exciton correlations, although the signatures of the correlations were convolved with other signals making the interpretation and analysis of high-order exciton correlations difficult. Recent advances in the generation of multiple, fully phase-coherent light fields have enabled direct observation of multiple-quantum coherences that directly reveal the correlations among multiple excitons using 2D FT OPT. For example, two phase-coherent light fields $\mathbf{E}_1(\mathbf{k_1})$ and $\mathbf{E}_2(\mathbf{k_2})$, where $\mathbf{k_i}$ are experimentally specified wave-vectors, can generate a two-quantum coherence at approximately twice the single-exciton frequency during a scanned time interval t_{2Q}; after this interval, a third phase-coherent light field $\mathbf{E}_3(\mathbf{k_3})$ can project the state into a single-quantum coherence which radiates, at a well defined wavevector $\mathbf{k}_{sig} = \mathbf{k_1} + \mathbf{k_2} - \mathbf{k_3}$, the phase-coherent signal field $\mathbf{E}_{sig}(\mathbf{k}_{sig})$ that is measured as a function of frequency ω_{em}. The projection depends on the phase of the two-quantum coherence, and therefore the emitted signal shows oscillations at the two-quantum frequency as the time interval t_{2Q} is scanned. Fourier transformation of the signal with respect to t_{2Q} reveals the two-quantum coherences from which the signal at ω_{em} was generated. With additional phase-related fields, higher-order multiple-quantum coherences and

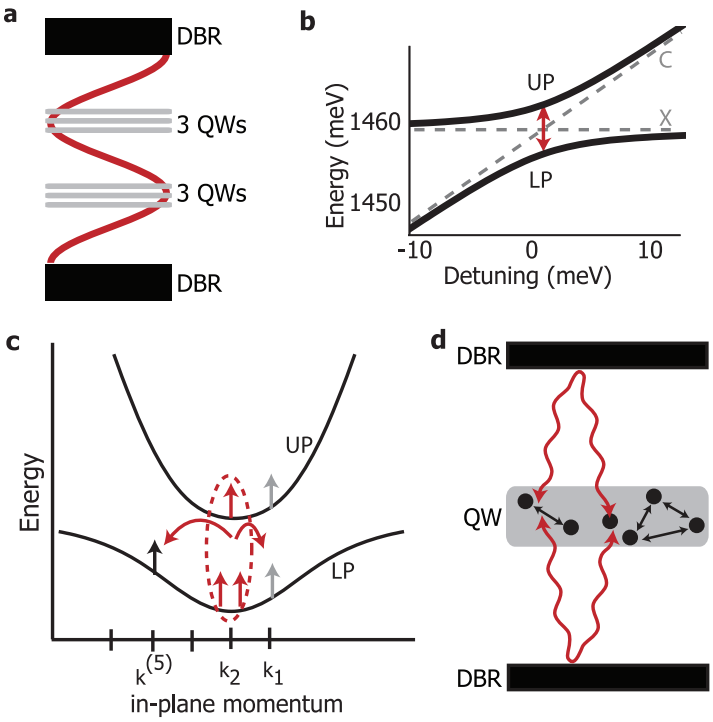

Figure 1. Exciton–polaritons in a SCMC. (a) A microcavity consisting of two distributed Bragg reflectors (DBRs) sandwiching two sets of three QWs. The cavity length is $\frac{3}{2}\lambda_X$, where λ_X is the QW exciton resonance wavelength. The QWs are placed at the antinodes of the standing wave in the cavity. (b) The energies of the exciton (X) and cavity (C) modes plotted as a function of energy detuning as the cavity length is varied (grey dashed lines). Strong coupling between X and C produce LP and UP states (black solid lines), exhibiting anti-crossing behaviour. The Rabi splitting is 7 meV, as given by the red double-sided arrow. (c) The energies of LP and UP plotted as a function of in-plane momentum. Three spin-up polaritons (red arrows) are excited by three interactions with field $\mathbf{E}(\mathbf{k_2})$, and their correlations through various coupling mechanisms (dashed red circle) result in a three-quantum coherence at $3\mathbf{k_2}$; after a variable delay t_{3Q}, a field at $\mathbf{E}(\mathbf{k_1})$ stimulates scattering, curved red arrows, into the $\mathbf{k_1}$ and $\mathbf{k^{(5)}} = 3\mathbf{k_2} - 2\mathbf{k_1}$ directions, resulting in two polaritons in the $\mathbf{k_1}$ state (grey) and one polariton in the $\mathbf{k^{(5)}}$ state (straight black arrow), along which the signal emerges. (d) Different types of coupling mechanisms between polaritons in a single QW embedded inside a microcavity. Polaritons (black circles) can be correlated through Coulomb interactions (straight black arrows), light fields (curvy red lines) or both.

multi-exciton correlations can be elucidated, e.g. three fields can be used to generate a three-quantum coherence, and after a scanned time delay t_{3Q}, two additional fields can be used to project into a single-quantum coherence that radiates the signal field. In GaAs QWs, two-quantum coherences at exactly twice the exciton frequencies were observed from correlated exciton pairs of the same spin [15], in addition to weakly bound biexciton [14]

and triexciton [16] correlations among excitons with mixed spins. Here, we report the direct resolution of up to four-polariton coherences contributing to UP and LP nonlinear emission. As will be shown, the spectral separation of various multi-polariton coherences is essential to clearly elucidate the role of multi-exciton correlations in polariton nonlinear interactions.

2. Methods

The sample structure was a GaAs SCMC with $In_{0.06}Ga_{0.94}As$ QWs embedded inside [1]. The cavity length was 3/2 times the exciton resonance wavelength of 850 nm. A set of three QWs, separated by 10 nm thick GaAs layers, were at the two antinodes. The cavity length was wedged slightly so that the cavity mode could be detuned relative to the exciton mode. The exciton–photon coupling strength, Ω, is 7 meV, as given by the LP and UP splitting at zero detuning. The cavity was surrounded by 17 (20) pairs of distributed Bragg reflectors consisting of $GaAs/Al_{0.18}Ga_{0.82}As$ at the top (bottom). Experiments were run with the sample at 10 K.

2D spectra were recorded using 2D spatial and temporal pulse shaping techniques through which the beam geometry and the relative phases and time delays of femtosecond pulses in the separate beams can all be controlled and varied without the need for realignment of mirrors or use of delay stages or interferometers, as previously reported [14, 16, 17]. Nonlinear signals, up to seventh order in the excitation fields, were generated using single or multiple field interactions of the pulses in two excitation beams, with wavevectors $\mathbf{k_2}$ and $\mathbf{k_1}$, pulse widths of 100 fs, and wavelengths centred at 850 nm. The beams were kept less than 2° from normal incidence. Using a pair of identical transmissive diffractive optics, a reference beam was directed around the sample and superimposed with the coherent signal beam that emerged from the sample at the phase-matched wavevector $2\mathbf{k_2} - \mathbf{k_1}$, $3\mathbf{k_2} - 2\mathbf{k_1}$ or $4\mathbf{k_2} - 3\mathbf{k_1}$ for third-, fifth- or seventh-order measurements, respectively. The dispersed frequency components of the signal field were measured through spectral interferometry. For third- and fifth-order spectra, the beam at $\mathbf{k_2}$ was kept horizontally polarized while the beam at $\mathbf{k_1}$ and the detection polarization were either co-circularly or cross-circularly polarized. Assuming that the spins of the polaritons in the final states ($\mathbf{k_{sig}}$ and $\mathbf{k_1}$) preserve the spins of the initially excited polaritons (in $\mathbf{k_2}$), this polarization scheme allows us to selectively detect the signal due to polaritons with the same spin (co-circular) or the signal due to polaritons where one has a spin opposite to the other(s). For seventh-order spectra, all beams were co-circularly polarized.

3. Results and discussion

In figure 2, we show two-quantum 2D spectra, where two-polariton coherences were excited by two time-coincident fields before a third field generates FWM nonlinear emission from a single polariton state. The polarizations of the excitation and reference beams are controlled so that the two initially excited polaritons that contribute to the signal have either the same spin or are spin-paired (see Methods section). The spectra show peaks representing excitation of different combinations of LP and UP: two LPs (LP_2), two UPs (UP_2) and a mixed combination of LP and UP (MP_2). The 2D spectra reveal how LP_2, UP_2 and MP_2 coherences contribute to the nonlinear signals at LP and UP frequencies: LP_2 and UP_2 emit into only LP or UP, respectively, but MP_2 emits into either LP or UP. Although the same two-polariton coherences are observed in same-spin or spin-paired spectra, there are dramatic differences in the relative intensities of the peaks which we characterize using a ratio, R, equal to the integrated intensity of MP_2 over

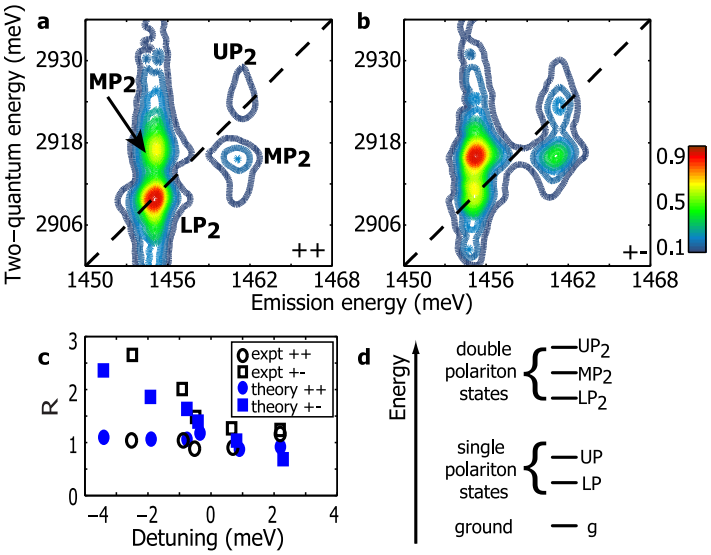

Figure 2. Two-quantum coherences. Experimental two-quantum 2D spectra, taken with the cavity resonance 1 meV lower than the exciton resonance, in the same-spin (a) or spin-paired (b) configuration, as described in the Methods section. Peaks on the diagonal dashed lines are LP_2 and UP_2 two-quantum coherences generated by the first two field interactions that emitted after the third field interaction from LP and UP single-quantum coherences, respectively. Off-diagonal peaks are MP_2 two-quantum coherences emitting from either LP or UP single-quantum coherences. (c) The ratio R, giving the integrated peak intensity of MP_2 over LP_2 as described in the text, is plotted as a function of the detuning of the cavity resonance from the exciton resonance. The ○-(□-)markers indicate experimental values of R for same-spin (spin-paired) 2D spectra and ●-(■-)markers indicate theoretical values of R for same-spin (spin-paired) 2D spectra. (d) Energy diagram showing the ground, single polariton and double polariton states.

the integrated intensity of LP_2. The integrated intensity is calculated along the two-quantum dimension at the LP emission energy and accounts for both the peak intensity and linewidth of each peak. For the spectra shown in figure 2, R is approximately one (two) for the same-spin (spin-paired) spectrum. The value of R also depends on the detuning of the cavity resonance from the exciton resonance, as shown in figure 2(c): the same-spin R is nearly constant whilst the spin-paired R varies from one to nearly three, taken over a range of detuning values ± 3 meV.

In order to understand the polarization and detuning dependence of R, 2D spectra were calculated following the calculations of 1D FWM spectra by Kwong *et al* [5, 19], as summarized in appendix A. In the calculations, contributions to the third-order polariton susceptiblity can be clearly identified: mean-field Coulomb repulsion and non-binding two-exciton Coulomb correlations contribute to the same-spin third-order susceptibility and only two-exciton Coulomb correlations contribute to the spin-paired third-order susceptibility [19]. Same-spin and spin-paired two-quantum 2D spectra are calculated for various detuning values, as shown in appendix A, and used to find values of R as a function of detuning, shown in figure 2(c). R is nearly one in the same-spin configuration but varies from one to over two

in the spin-paired configuration, over detuning values similar to the experimental values. The calculations confirm the spin-dependent contributions to the 2D spectra in figure 2, including two-exciton correlations.

The dramatic detuning dependence of the spin-paired R can be attributed to biexciton correlations. As the cavity detuning is varied, LP_2 and MP_2 move in or out of resonance with the biexciton energy and become more or less strongly correlated through a biexciton interaction. Specifically, as the cavity energy is lowered and the LP becomes more light-like, the LP_2 energy moves out of resonance with the biexciton until biexciton interactions no longer correlate two LPs. Because the UP becomes exciton-like as the cavity energy is lowered, biexciton interactions can correlate MP_2 much more than LP_2 for negative detunings. In fact, for negative detunings in the spin-paired configuration, correlations between LP and UP are the main source of nonlinear signal. Although the same-spin Coulomb correlation strength is also frequency dependent, the correlation strength is not sharply peaked (note that there is no bound biexciton state for two same-spin excitons) but increases relatively gradually with negative detuning frequency [19]. At least for the detuning values in figure 2(c), the frequency dependence of the same-spin Coulomb correlations does not cause strong frequency dependence in the strength of polariton nonlinear interactions. Regardless of the spin configuration, the relative nonlinear signal strengths at LP or UP depend on the strengths of the LP_2, UP_2 and MP_2 correlations which are normally integrated over in typical FWM experiments [18]. By clearly separating the LP_2 and MP_2 coherences, we are able to directly resolve the role of the biexciton correlation in polariton nonlinear dynamics.

Polariton nonlinear dynamics may also be mediated by higher-order correlations. In bare GaAs QWs, three excitons have recently been shown to correlate into a bound triexciton state if the spin of one of the excitons is opposite to the other two [16]. Coulomb correlations among three excitons of the same spin or four excitons of any spin combination were not observed. Other work studying QWs using six-wave mixing has shown that the biexciton and exciton may mix, and even correlate [22, 23]. As far as the authors are aware, there have been no reported observations of correlations or coherent mixing between three or more excitons of the same spin in bare exciton systems. If polariton interactions were mediated only by exciton nonlinearities, then triexciton correlations and biexciton–exciton mixing should mediate three-polariton coherences and no coherences of three or more polaritons with the same spin should be observed. However, as shown in figures 3 and 4, we can detect three-quantum and four-quantum coherences in the six-wave mixing and eight-wave mixing directions, respectively, including coherences between polaritons of the same spin. The 2D spectra show peaks representing various combinations of LP and UP with the same spin (figures 3(a) and 4) and with one spin opposite the others (figure 3(b)). In the three-quantum spectra, mixed polariton coherences (LP_2UP) are again stronger relative to the pure LP coherence (LP_3) if one spin is opposite to the others.

In addition to high-order Coulomb correlations, the high-order multiple polariton coherences we observe may occur through multiple third-order exciton nonlinearities. A $2k_2 - k_1$ polariton generated from third-order exciton nonlinearities can interact with two polaritons that are directly excited by the k_2 and k_1 input fields to generate a $3k_2 - 2k_1$ polariton with a fifth-order dependence on the input fields [20, 21]. The fifth-order polariton can interact with two more first-order polaritons in yet another third-order process, yielding a seventh-order $4k_2 - 3k_1$ signal and so on. The coupling of two-exciton Coulomb correlations with a third polariton through the cavity mode is shown on the left side of figure 1(d). Such 'cascaded'

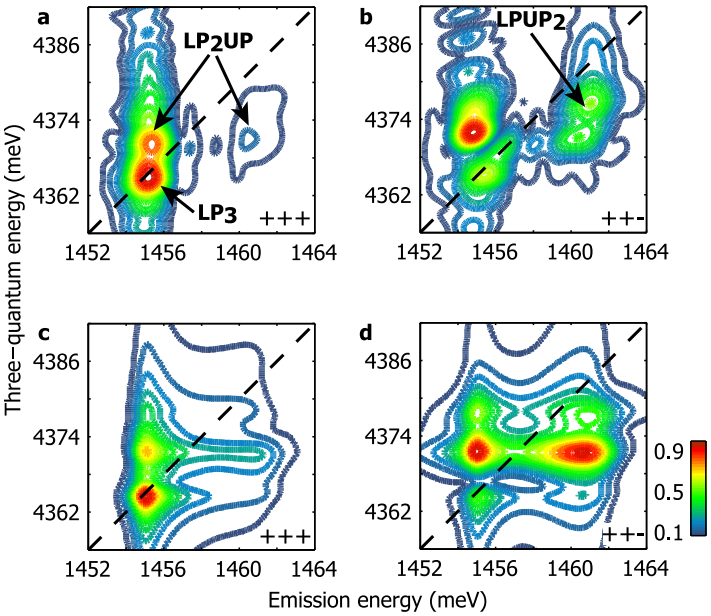

Figure 3. Three-quantum coherences. (a), (b) Experimental three-quantum 2D spectra taken with the cavity resonance 1 meV lower than the exciton resonance. The spectra show correlations among three LPs (LP_3) and two LPs with one UP (LP_2UP) emitting into LP. LP_2UP and a correlation between one LP and two UPs ($LPUP_2$) emit into UP. All three polaritons have the same spin in (a) and one is opposite the other two in (b). (c), (d) Calculated three-quantum 2D spectra matching the experimental conditions in figures 3(a) and (b), respectively.

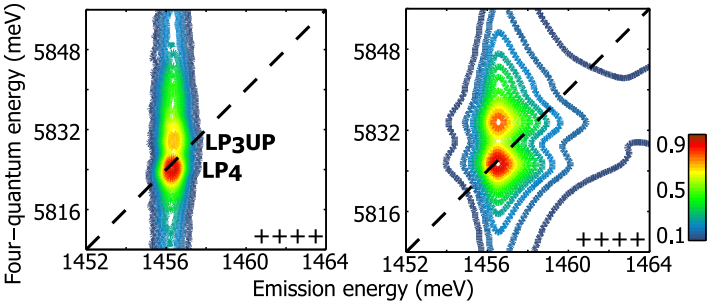

Figure 4. Four-quantum coherences. (a) Experimental 2D spectra taken with the cavity resonant with the exciton energy showing four-quantum coherences emitting into the LP state. All polaritons have the same spin. (b) Calculated 2D spectra matching the experimental conditions. From bottom to top, coherences are observed among four LPs (LP_4) and among three LPs and one UP (LP_3UP).

third-order signals were not observed in bare QWs but have been observed in bulk samples [16, 24, 25]. The signals represent sequential interactions mediated by emitted fields propagating through the sample, with no influence on the earlier exciton participants by the later ones, rather than interactions that mutually influence and correlate all the excitons involved. In microcavities, a coherent exciton–polariton field can play a similar role in generating a new

high-order coherence, but instead of leaving the sample, the field components are confined and continue to interact with the electronic coherences, mutually correlating them. In other words, the two coherences are mutually influenced and correlated through their associated fields, and the signal that emerges from the sample represents a true multi-exciton–polariton correlation that we will denote as 'field-coupled' (see appendix B for more discussion).

We calculated fifth-order 2D spectra for the same-spin and mixed-spin configurations, figures 3(c) and (d). The 2D spectra were calculated by coupling five polaritons with two third-order exciton interactions, as described in appendix A. The calculated 2D spectra qualitatively reproduce the experimental results. In particular, the relative strengths of LP_3 and LP_2UP for the two spin configurations are well reproduced, indicating that two coupled third-order interactions may explain the polarization dependence of the fifth-order 2D spectra. In the mixed-spin spectra, for example, a LP and UP interact strongly through biexciton attraction, and additional Coulomb interactions with a second LP coherence gives the relatively strong peak observed at LP_2UP. The seventh-order 2D spectra for the same-spin configuration are calculated by field-coupling of seven polaritons through three third-order exciton interactions. The results are shown in figure 4(b). Again the calculations qualitatively reproduce the experimental 2D spectrum: the emission from UP is diminished and correlations involving at least three LPs are the strongest features.

Based on these calculations, we cannot exclude contributions from high-order Coulomb correlations to high-order polariton correlations. As previously mentioned, triexciton interactions should mediate correlations between three polaritons with mixed spins. Considering a total binding energy of approximately 3 meV [16], triexciton interactions would be the strongest for LP_2UP at the detuning shown in figure 3. Triexciton interactions would therefore give qualitatively similar correlation strengths as field-coupled third-order exciton–polariton nonlinear interactions. Careful calculations of the triexciton binding energy should help separate the field-coupled and high-order Coulomb contributions to the three-quantum coherences, but such calculations remain at or beyond the limit of current theoretical capabilities [26]. Additionally, although unbound three-exciton or four-exciton correlations were not observed in bare QWs, unbound three-exciton or four-exciton correlations may still play a role between polaritons because the high-order Coulomb and field-coupled correlations should be frequency dependent, just as the two-exciton correlation is frequency-dependent. Full understanding of the origins of these high-order multi-polariton coherences will require further theoretical work describing the high-order correlation functions. Additional experiments could be conducted with the k_2 and/or k_1 field interactions separated into different beams so that wavevector combinations that are resonant with both biexciton and high-order correlations could be examined. Five-quanta and higher-order multiple-quantum coherences also should be explored.

4. Conclusion

Using 2D spectroscopy we directly resolve how multipolariton correlations contribute to nonlinear signals. We are able to clearly demonstrate that the strong coupling to light modifies two-exciton correlations by tuning the oscillation frequencies of the constituent polaritons: depending on the spectral overlap with the biexciton resonance, two spin-paired polaritons can become strongly correlated through biexciton Coulomb interactions. In particular, for negative detunings and spin-paired polaritons, correlations between the LP and UP are the dominant sources of nonlinear emission from the LP state. The ability to control the nonlinear LP signal

by exploiting the correlations with the UP could be an interesting mechanism for nonlinear devices. Additionally, correlations among up to four polaritons are observed, a higher order than observed in bare QWs, demonstrating that high-order correlations can be mediated through the polariton fields. The maximum order of the Coulomb correlations cannot be clearly elucidated: multiple third-order Coulomb interactions, coupled through the cavity light field, give calculated correlation signals that are qualitatively similar to the experimental spectra, but high-order Coulomb correlations may still contribute to the observed multi-exciton–polariton signals. Further theoretical work detailing the exact nature of these correlations should inform future experiments and devices exploiting polariton nonlinearities.

Acknowledgments

The authors thank John Roberts for sample fabrication. GC and JBB were supported by UK EPSRC grants EP/G060659/1 and EP/F011393 and the EU grants CLERMONT4, PITNGA-2009-235114 and INDEX FP7-2011-289968. PW was supported as part of the Center for Excitonics, an Energy Frontier Research Center funded by the US Department of Energy, Office of Science, Office of Basic Energy Sciences under Award Number DE-SC0001088.

Appendix A. Calculations of two-dimensional spectra

In this section, we describe in detail our method to calculate third-order and field-coupled fifth-order 2D spectra for a sample structure consisting of a single QW embedded inside a SCMC. Although the sample structure is slightly different than the structure used in the experiments, the calculations qualitatively reproduce key features in the 2D spectra. We first briefly review how to calculate FWM signals in a model structure and show how to calculate third-order 2D spectra. We then describe and calculate the fifth-order and seventh-order polariton correlations.

FWM signals are calculated following the work of Kwong *et al* [5, 19]. The calculations have been described in detail and we only provide a brief summary here. Assuming classical light fields, propagation of light through the SCMC structure can be solved using the following wave equation:

$$\left[n^2(z,\omega)\frac{\omega^2}{c^2}+\frac{\partial^2}{\partial z}\right]\mathbf{E}(z,\omega)=-4\pi\frac{\omega^2}{c^2}\mathbf{P}(z,\omega), \tag{A.1}$$

where $n(z,\omega)$, $\mathbf{E}(z,\omega)$ and $\mathbf{P}(z,\omega)$ are the refractive index, electric field and polarization at each position along the z-axis, normal to the QW plane. Except for the QW layer, the propagation through the SCMC can easily be solved using standard transfer matrix calculations. The key challenge is calculation of the nonlinear polarization generated in the QW, which acts as a source term on right-hand side of (A.1).

The third-order polarization is calculated by standard perturbation theory. In the frequency domain, the third-order polarization at the position of the QW is given by [27]:

$$\mathbf{P}_l^{(3)}(\omega)=\frac{1}{(2\pi)^2}\sum_{m,n,p}\int \mathrm{d}\omega_1\,\mathrm{d}\omega_2\,\mathrm{d}\omega_3\delta(\omega_1+\omega_2-\omega_3-\omega)\chi^{(3)}_{lmnp}(\omega_1,\omega_2,\omega_3)$$
$$E_{Qm}(\omega_1)E_{Qn}(\omega_2)E^*_{Qp}(\omega_3), \tag{A.2}$$

where $\chi^{(3)}_{lmnp}$ is the third-order exciton susceptibility describing interactions between excitons in the m, n and p spin states contributing to the polarization in the spin state l. The electric fields

in (A.2) are not the applied fields external to the SCMC, but are the electric fields at the position of the QW, which have peaks at the LP and UP resonances.

Microscopic calculation of the third-order susceptibility is extremely challenging because of the many-body Coulomb interactions. Kwong *et al* [19] calculated the susceptibility using the dynamics-controlled truncation approach giving the result:

$$\chi^{(3)}_{mn}(\omega_1, \omega_2, \omega_3) = -\frac{\chi^{(1)}(\omega_1)\chi^{(1)}(\omega_2)\chi^{(1)*}(\omega_3)\chi^{(1)}(\omega_1+\omega_2-\omega_3)}{q_e^4|\langle d\rangle|^4|\phi(0)|^4}$$
$$\left[\delta_{mn}G^{\mathrm{PSF}}(\omega_1, \omega_2) + T_{mn}(\omega_1+\omega_2)\right], \tag{A.3}$$

where $\chi^{(1)}(\omega)$ is the first-order exciton susceptibility, q_e is the magnitude of the charge of an electron, $\langle d\rangle$ is the transition dipole matrix element and $\phi(0)$ is the exciton wavefunction at $\mathbf{k}=0$. $G^{\mathrm{PSF}}(\omega_1, \omega_2)$ is the phase-space filling contribution, i.e. the decrease in absorption due to occupation of the exciton state. In all calculations, we use values of $\langle d\rangle\phi(0) = 0.035$, consistent with [19]. The last term, T_{mn}, gives the Coulomb interactions and depends on the spin configuration, mn:

$$T_{++}(\Omega) = V^{\mathrm{HF}} + 2G_+(\Omega), \tag{A.4}$$

$$T_{+-}(\Omega) = G_+(\Omega) + G_-(\Omega), \tag{A.5}$$

where + and − denote spin up and spin down, V^{HF} is the frequency-independent mean-field Coulomb interaction and $G_m(\Omega)$ is the frequency-dependent two-exciton Coulomb correlation.

The frequency dependence of T_{nm} depends significantly on the spin configuration, as shown by Kwong *et al* [19]. There is a sharp peak in T_{+-} at the biexciton resonance, approximately 2 meV below twice the bare exciton resonance for a GaAs sample [19]. Although T_{++} increases with frequency beginning at roughly twice the bare exciton energy due to the increasing density of states, there is no similar resonance in its spectrum. Based on equations (A.3)–(A.5), $\chi^{(3)}$ has contributions from phase-space filling, mean-field Coulomb repulsion and two-exciton Coulomb correlations in the same-spin configuration but only contributions from two-exciton Coulomb correlations in the spin-paired configuration. By inserting equations (A.2)–(A.5) into (A.1), the transmitted third-order electric field can be computed for different spin configurations. The frequency-dependent values of T_{nm} and $G^{\mathrm{PSF}}(\omega_1, \omega_2)$ used in all calculations are given by [19].

A full 2D spectrum can be calculated by variably delaying the excitation fields in (A.2). A time delay, τ, of the electric fields is given by a linear phase sweep in the frequency domain:

$$E(\omega) = g(\omega) \times \exp[\mathrm{i}(\omega-\omega_c)\tau], \tag{A.6}$$

where ω_c is a carrier frequency that sets the centre of the phase sweep and $g(\omega)$ is the Gaussian envelope of the pulse. Conveniently, time delays in the experiment are generated in the frequency domain by a pulse shaper, exactly as indicated in (A.6), with an experimentally chosen carrier frequency [17]. (A.6) is inserted into (A.2) and the transmitted third-order electric field is calculated for time delays between the two time-coincident non-conjugate fields, E_1 and E_2, and the third, conjugate field, E_3. Fourier transformation along the scanned time delay dimension gives the 2D spectra shown in figure A.1.

There are two mechanisms for fifth-order signal to be generated in exciton systems: two coupled third-order exciton correlations or a fifth-order exciton correlation. For the case of two

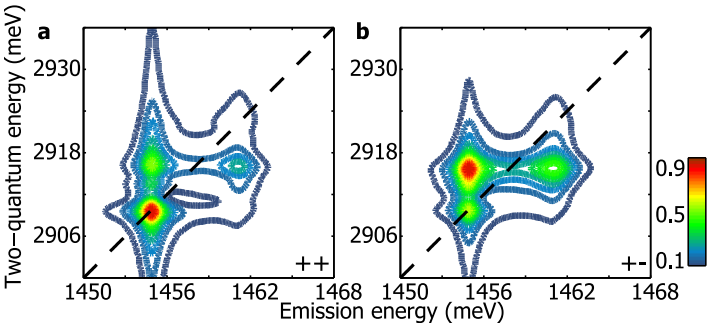

Figure A.1. Calculated two-quantum coherences. (a), (b) Calculated two-quantum 2D spectra in the same-spin (a) and spin-paired (b) configurations matching the experimental conditions in figures 1(a) and (b), respectively.

field-coupled third-order exciton interactions, the fifth-order polarization is given by:

$$\mathbf{P}^{(5)}_{\text{field},l}(\omega) = \frac{1}{(2\pi)^2}\sum_{m,n,p}\int \mathrm{d}\omega_1\,\mathrm{d}\omega_2\,\mathrm{d}\omega_3\delta(\omega_1+\omega_2-\omega_3-\omega)\chi^{(3)}_{lmnp}(\omega_1,\omega_2,\omega_3)$$
$$E^{(3)}_{Qm}(\omega_1)E^{(1)}_{Qn}(\omega_2)E^{(1)*}_{Qp}(\omega_3). \tag{A.7}$$

The fifth-order polarization in (A.7) is generated by two third-order exciton interactions; one third-order interaction generates the polariton given by the $E^{(3)}_{Qm}$ term, the other third-order interaction couples this polariton with two other polaritons directly excited by the external fields. Crucially, all interactions described in (A.7) occur at the position of the QW. Normally, first-order coherences in thin QWs do not couple to third-order fields emitted from the same QW samples [16], but in a microcavity structure the fields are confined and can continue to interact at the QW layer. In bulk samples, sequential cascaded interactions also generate fifth-order signal similar to the signal described in (A.7) but at different positions in the sample [20, 21]; the third-order field generated at one position of the sample propagates along the sample, interacting with the first-order excitation fields as it arrives at different positions on the sample.

The field-coupled signals emitted from microcavities are fundamentally different from sequential cascades from bulk samples. In the microcavity case, the field components are not just the incident fields but dynamic polariton fields. The correlated nature of the coupled third-order exciton interactions may not be obvious from (A.7). This is because the electric fields in (A.7) are treated semiclassically [5, 19]; the electric field operators and the exciton operators have been factorized and the former written as a classical field. The consequence of this formulation is that the electric fields are not actually influenced by the exciton correlations. However, considering the confinement by the microcavity, the quantum nature of the electric field should be important in nonlinear experiments. The effects of quantum correlation and semiclassical factorization were first elucidated by Savasta and Girlanda [9] and more recently extended to higher-orders by Portolan *et al* [28]. In these works, the electric field is described by its own dynamic equation and is correlated to the exciton through Pauli-blocking interaction [9]. This correlation, in turn, is mutually influenced by both multi-exciton correlations and multi-photon cavity correlations. Two-exciton–photon correlations have been demonstrated by measuring correlated intensity fluctuations in twin beams generated by FWM in a SCMC [29]. Despite the role of quantum correlations, the application of the semiclassical approximation in (A.7)

should not detrimentally affect our ability to compare qualitative characteristics (e.g. relative peak intensities) between the fifth-order signal calculated by (A.7) and the experimental fifth-order signal since such characteristics are usually given by the exciton correlations described in $\chi^{(3)}$. For certain experimental configurations (e.g. if the Rabi-splitting is equal to the biexciton binding energy) [30, 31], the multi-exciton correlations become strongly dressed by the multi-photon states, significantly altering the lineshapes and energies of the multi-polariton correlations, but the sample used in our experiments does not appear to show these effects (see next section for more discussion).

Fifth-order polarizations may also be generated by fifth-order Coulomb interactions. In this case, the polarization is given by:

$$\mathbf{P}^{(5)}_{\mathrm{coul},l}(\omega) = \frac{1}{(2\pi)^2}\sum_{j,k,l,m,n}\int \mathrm{d}\omega_1\,\mathrm{d}\omega_2\,\mathrm{d}\omega_3\delta(\omega_1+\omega_2+\omega_3-\omega_4-\omega_5-\omega)$$
$$\chi^{(5)}_{lmnpqr}(\omega_1,\omega_2,\omega_3,\omega_4,\omega_5)E_{Qm}(\omega_1)E_{Qn}(\omega_2)E_{Qp}(\omega_3)E^*_{Qq}(\omega_4)E^*_{Qr}(\omega_5). \quad \text{(A.8)}$$

The fifth-order exciton susceptibility in (A.8) accounts for three-exciton Coulomb correlations such as bound triexciton interactions. Fifth-order electric fields will be generated by both P_{field} and P_{coul} and propagate outside the sample using (A.1). Unfortunately, calculation of the fifth-order exciton susceptibility, including all Coulomb correlations, is extremely challenging and outside the scope of this paper so only P_{field} is included in the calculations. Full 2D spectra are calculated as described above and shown in figures 3(c) and (d).

Seventh-order nonlinear signals can be generated through similar mechanisms: three coupled third-order exciton interactions, a third-order exciton interaction coupled to a fifth-order interaction, and a seventh-order exciton interaction can all contribute signal in the seventh-order direction. Without a calculation of the fifth-order or seventh-order exciton susceptibility, however, only the contribution from three coupled third-order exciton interactions can be calculated:

$$\mathbf{P}^{(7)}_{\mathrm{field},l}(\omega) = \frac{1}{(2\pi)^2}\sum_{m,n,p}\int \mathrm{d}\omega_1\,\mathrm{d}\omega_2\,\mathrm{d}\omega_3\delta(\omega_1+\omega_2-\omega_3-\omega)\chi^{(3)}_{lmnp}(\omega_1,\omega_2,\omega_3)$$
$$E^{(5)}_{\mathrm{field},Qm}(\omega_1)E_{Qn}(\omega_2)E^*_{Qp}(\omega_3), \quad \text{(A.9)}$$

where $E^{(5)}_{\mathrm{field},Qm}$ is the field at the QW due to the polarization from (A.7). The two coupled third-order exciton interactions calculated in (A.7) are coupled to two other polaritons through another third-order exciton interaction. Full 2D spectra are calculated using (A.9) and shown in figure A.1(b).

Appendix B. Discussion of multi-exciton strong coupling

There has been some work detailing how biexcitons may become strongly coupled to the cavity light field. Although the biexciton itself does not directly couple to light, FWM experiments have shown that the exciton-to-biexciton transition may become strongly coupled to the light mode when the exciton transition becomes saturated [32, 33]. Since we work at the perturbative limit, keeping our excitation powers at least an order of magnitude lower than the saturation threshold, such effects are not observed in our results. The highest powers used

in our experiments, for the seventh-order spectra, show a seventh-order dependence on the field strengths, confirming that we are below the saturation point.

Additionally, the possibility exists that the biexciton can couple to two-photon cavity modes, forming what is often described as a bipolariton. Normally, such coupling does not lead to significant changes in biexciton energy or linewidth since the biexciton interaction occurs over a much larger k-space range than that within which the cavity light field is coupled to the exciton [34, 35]. However, some work has demonstrated the existence of a bipolariton state when the biexciton binding energy is equal to the Rabi splitting of the cavity [30, 31], as mentioned above. Light fields can also couple to the biexciton when considering the bulk (or zero-order) photon modes [36], although such effects are not unique to microcavities. A two-qauntum 2D spectrum should provide a sensitive probe to the bipolariton dispersion or detuning dependence. However, for our specific sample, the Rabi-splitting (7 meV) is most likely several times larger than the biexciton binding energy (2 meV in GaAs) [14] and we do not observe shifts in energy in the positions of LP_2, MP_2 or UP_2 that we can attribute to bipolaritons.

References

[1] Savvidis P G, Baumberg J J, Stevenson R M, Skolnick M S, Whittaker D M and Roberts J S 2000 Angle-resonant stimulated polariton amplifier *Phys. Rev. Lett.* **84** 1547–50

[2] Kasprzak J *et al* 2006 Bose–Einstein condensation of exciton polaritons *Nature* **443** 409–14

[3] Utsunomiya S *et al* 2008 Observation of Bogoliubov excitation in exciton–polariton condensates *Nature Phys.* **4** 700–5

[4] Savasta S, Stefano O D and Raffaello G 2003 Many-body and correlation effects on parametric polariton amplification in semiconductor microcavities *Phys. Rev. Lett.* **90** 096403

[5] Kwong N H, Takayama R, Rumyantsev I, Kuwata-Gonokami M and Binder R 2001 Evidence of nonperturbative continuum correlations in two-dimensional exciton systems in semiconductor microcavities *Phys. Rev. Lett.* **87** 027402

[6] Chemla D S and Shah J 2001 Many-body and correlation effects in semiconductors *Nature* **411** 549–57

[7] Weisbuch C, Nishioka M, Ishikawa A and Arakawa Y 1992 Observation of the coupled exciton–photon mode splitting in a semiconductor quantum microcavity *Phys. Rev. Lett.* **69** 3314–7

[8] Houdré R, Weisbuch C, Stanley R P, Oesterle U, Pellandini P and Llegems M 1994 Measurement of cavity-polariton dispersion curve from angle-resolved photoluminescence experiments *Phys. Rev. Lett.* **73** 2043–6

[9] Savasta S and Girlanda R 1996 Quantum optical effects and nonlinear dynamics in interacting electron systems *Phys. Rev. Lett.* **77** 4736–9

[10] Östriech Th, Schönhammer K and Sham L J 1995 Exciton–exciton correlation in the nonlinear optical regime *Phys. Rev. Lett.* **74** 4698–701

[11] Axt V M, Kuhn T, Haase B, Neukirch U and Gutowski J 2004 Estimating the memory time induced by exciton–exciton scattering *Phys. Rev. Lett.* **93** 127402

[12] Li X, Zhang T, Borca C N and Cundiff S T 2006 Many-body interactions in semiconductors probed by optical two-dimensional Fourier transform spectroscopy *Phys. Rev. Lett.* **96** 057406

[13] Zhang T, Kuznetsova I, Meier T, Li X, Mirin R P, Thomas P and Cundiff S T 2007 Polarization-dependent optical 2D Fourier transform spectroscopy of semiconductors *Proc. Natl Acad. Sci. USA* **104** 14227–32

[14] Stone K W, Gundogdu K, Turner D B, Li X, Cudiff S T and Nelson K A 2009 Two-quantum 2D FT electronic spectrosocpy of biexcitons in GaAs quantum wells *Science* **324** 1169–73

[15] Karaiskaj D, Bristow A D, Yang L, Dai X, Mukamel S and Cundiff S T 2010 Two-quantum many-body coherences in two-dimensional Fourier-transform spectra of exciton resonances in semiconductor quantum wells *Phys. Rev. Lett.* **104** 117401

[16] Turner D B and Nelson K A 2010 Coherent measurements of high-order electronic correlations in quantum wells *Nature* **466** 1089–92
[17] Turner D B, Stone K W, Gundogdu K and Nelson K A 2011 The coherent optical laser beam recombination technique (COLBERT) spectrometer: coherent multidimensional spectroscopy made easier *Rev. Sci. Instrum.* **82** 081301
[18] Jonas D M 2003 Two-dimensional femtosecond spectroscopy *Annu. Rev. Phys. Chem.* **54** 425–63
[19] Kwong N H, Takayama R, Rumyantsev I, Kuwata-Gonokami M and Binder R 2003 Third-order exciton-correlation and nonlinear cavity–polariton effects in semiconductor microcavities *Phys. Rev.* B **64** 045316
[20] Ulness D J, Kirkwood J C and Albrecht A C 1998 Competitive events in fifth order time resolved coherent Raman scattering: direct versus sequential processes *J. Chem. Phys.* **108** 3897–902
[21] Blank D A, Kaufman L J and Fleming G R 1999 Fifth-order two-dimensional Raman spectra of CS_2 are dominated by third-order cascades *J. Chem. Phys.* **111** 3105–14
[22] Bolton S R, Neukirch U, Sham L J, Chemla D S and Axt V M 2000 Demonstration of sixth-order Coulomb correlations in a semiconductor single quantum well *Phys. Rev. Lett.* **85** 2002–5
[23] Langbein W, Meier T, Koch S W and Hvam J M 2001 Spectral signatures of χ^5 processes in four-wave mixing of homogenously broadened excitons *J. Opt. Soc. Am.* B **18** 1318–25
[24] Pantke K H, Schillak P, Razbirin B S, Lyssenko V G and Hvam J M 1993 Nonlinear quantum beats of propagating polaritons *Phys. Rev. Lett.* **70** 327–30
[25] Schulze A, Knorr A and Koch S W 1995 Pulse propagation and many-body effects in semiconductor four-wave mixing *Phys. Rev.* B **51** 10601–9
[26] Östreich T 2001 Higher-order Coulomb correlation in the nonlinear optical response *Phys. Rev.* B **64** 245203
[27] Cho M 2009 *Two-Dimensional Optical Spectroscopy* (Boca Raton, FL: Taylor and Francis)
[28] Portolan S, Di Stefano O, Savasta S, Rossi F and Girlanda R 2008 Dynamics-controlled truncation scheme for quantum optics and nonlinear dynamics in semiconductor microcavities *Phys. Rev.* B **77** 195305
[29] Romanelli M, Leyder C, Karr J Ph, Giacobino E and Bramati A 2007 Four wave mixing oscillation in a semiconductor microcavity: generation of two correlated polariton populations *Phys. Rev. Lett.* **98** 106401
[30] Baars T, Dasbach G, Bayer M and Forchel A 2001 Biexciton states in semiconductor microcavities *Phys. Rev.* B **63** 165311
[31] Oka H and Ishihara H 2008 Highly efficient generation of entangled photons by controlling cavity bipolariton states *Phys. Rev. Lett.* **100** 170505
[32] Saba M, Quochi F, Ciuti C, Oesterle U, Staehli J L, Deveaud B, Bongiovanni G and Mura A 2000 Crossover from exciton to biexciton polaritons in semiconductor microcavities *Phys. Rev. Lett* **85** 385–8
[33] Neukirch U, Bolton S R, Fromer N A, Sham L J and Chemla D S 2000 Polariton–biexciton transitions in a semiconductor microcavity *Phys. Rev. Lett.* **84** 2215–8
[34] La Rocca G C, Bassani F and Agranovich V M 1998 Biexcitons and dark states in semiconductor microcavities *J. Opt. Soc. Am.* B **15** 652–60
[35] Borri P, Langbein W, Woggon U, Esser A, Jensen J R and Hvam J M 2003 Biexcitons in semiconductor microcavities *Semicond. Sci. Technol.* **18** S351–60
[36] Ivanov A L, Borri P, Langbein W and Woggon U 2004 Radiative corrections to the excitonic molecule in GaAs microcavities *Phys. Rev.* B **69** 075312